

Nanomechanical thermal analysis of electrospun polymer fibers

Wei Wang, Andrew J. Bushby, and Asa H. Barber^{a)}

Department of Materials and Centre for Materials Research, Queen Mary, University of London, Mile End Road, London E1 4NS United Kingdom

(Received 11 August 2008; accepted 3 November 2008; published online 20 November 2008)

Thermomechanical properties of individual electrospun semicrystalline polyethylene oxide (PEO) fibers were measured using atomic force microscopy based indentation. Fibers showed a higher elastic modulus than corresponding films despite a lower crystallinity, indicating significant molecular alignment along the principle fiber axis. Heating of the fibers gave a progressive loss in elastic modulus highlighting a dominant amorphous thermomechanical response. This is in contrast to softening of an amorphous phase and melting of a crystalline phase in semicrystalline bulk PEO films. © 2008 American Institute of Physics. [DOI: 10.1063/1.3033222]

Electrospinning¹ is an important process for the manufacture of polymer fibers with some literature indicating that the mechanical properties of the electrospun fibers are superior to larger bulk equivalents.² As with other polymer fibers such as pultrusion, extrusion, and gel spinning, the resultant structural anisotropy is particularly effective for improving the mechanical properties along the fiber length and has led to a number of commercially available high strength, high stiffness fibrous materials. Structural characterization using x-ray diffraction indicates that preferential polymer orientation occurs in the electrospun fibers³ although there is some evidence to show that this results in little mechanical improvement.⁴ Arinstein *et al.*⁵ also suggested that supramolecular structures consisting of orientated amorphous polymer chains within polymer nanofibers dominate their mechanical properties. The structural organization is therefore critical for defining the mechanical properties yet is still not fully understood in electrospun polymer fibers. In this work, we use atomic force microscopy (AFM) to measure the mechanical properties of individual electrospun semicrystalline polymers over a range of temperatures using an indentation approach. Indentation has previously been applied to electrospun fibers⁶ but the nanomechanical thermal analysis (nMTA) in this work is particularly powerful as the mechanical response with temperature can reveal structural characteristics.

Polyethylene oxide (PEO) is a semicrystalline polymer that has been previously extensively used in electrospinning due to the ease of preparing the aqueous polymer solutions required for the electrospinning process.⁷ Electrospinning followed previous work by spinning from a 5.0 wt/v % polymer solution, using PEO powder ($M_w = 1\,000\,000$ g/mol, Sigma-Aldrich) dissolved in a 1:3 volume ratio of distilled water and ethanol at room temperature, to produce continuous fibers with a diameter of 477 ± 100 nm. For comparison, the same aqueous solution was cast onto a polystyrene (PS) Petri dish and dried at room temperature to form the equivalent films with a thickness of many hundreds of microns. The melting behavior of an electrospun PEO fiber mat and a solution cast PEO film was examined using differential scanning calorimetry (DSC) (not

shown), and the endothermic melting peak of the electrospun PEO fiber mat was found to have a melting temperature (T_m) of 64 °C, which was lower than the equivalent polymer film of 69 °C. The enthalpy (ΔH) of melting for the fiber mat and film was 132.6 and 168.2 J g⁻¹, respectively, from numerical integration of the area under the DSC melting peak. Comparison of ΔH with a purely crystalline PEO sample⁸ indicates that the crystal volume of 62.1% for the electrospun fibers was lower than the crystallinity of 78.8% in the PEO film. The decrease in both T_m and ΔH of the electrospun PEO fiber mat relative to the film highlights the lower crystal content produced from electrospinning as has been shown previously.⁶ This is further supported by previous work showing that the time required for fiber formation in electrospinning is relatively short,⁹ which hinders the development of crystalline structure.

The thermomechanical properties of individual PEO fibers were examined directly using AFM to image and mechanically test individual fibers over a range of temperatures. The selection of individual fibers is considered superior to the measurements of fiber mats due to the averaging that occurs over a range of fiber diameters. nMTA was carried out using an AFM combined within a heating chamber (NT-MDT, Rus.) with cantilever deflection monitored by an external optical setup. This design in combination with a closed-loop system provides very low drift measurements less than 10 nm °C⁻¹ and ensures that the AFM probe is of the same temperature as the sample. PEO fibers were electrospun onto a silicon substrate and imaged with AFM from room temperature to 70 °C with a heating rate comparable to the DSC studies of 5 °C min⁻¹. Figure 1 shows AFM images of an individual electrospun fiber during the heating process.

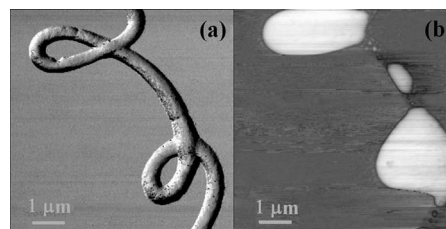


FIG. 1. AFM phase images of a single electrospun PEO fiber observed at (a) 23 °C and (b) 65 °C, showing the change from a solid cylindrical fiber to liquid droplets.

^{a)} Author to whom correspondence should be addressed. Electronic mail: a.h.barber@qmul.ac.uk.

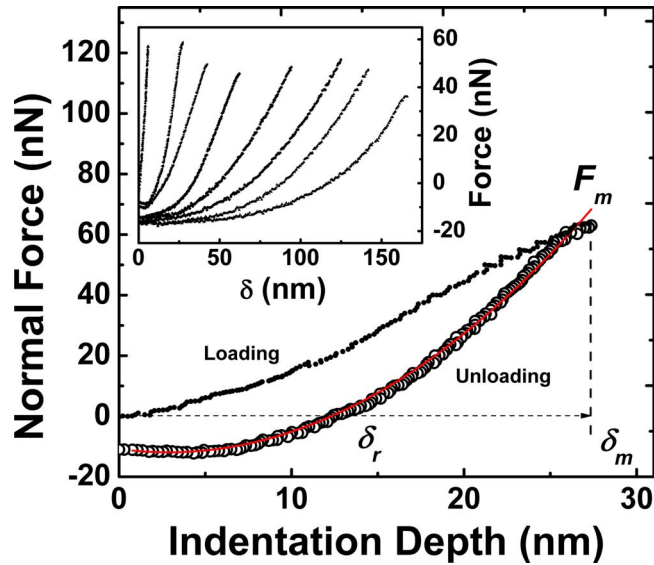


FIG. 2. (Color online) Plot of the loading-unloading normal force-indentation depth ($F-\delta$) for the indentation of an electrospun PEO fiber at 40 °C showing the fitting curve ($R^2=0.99$) with the theoretical $F-\delta$ dependence of Eq. (1). δ_m is the maximum indentation depth observed by the maximum applied force F_m and δ_r was taken at the intersection of the unloading $F-\delta$ curve and the zero axis. Inset shows the observed unloading $F-\delta$ curves of this PEO fiber over a range of temperatures from 23 to 40, 50, 55, 58, 60, 61.5, until 63 °C (left to right), indicating an increased δ with increasing fiber temperature under similar applied force.

The fiber changed from a cylindrical to hemispherical droplet geometry above 60 °C indicating Rayleigh instability. This is expected as the increasing thermal motion of the polymer chains allows minimization of the surface area from a cylindrical fiber to a droplet. Evaluation of the thermomechanical response of individual fibers at a specific temperature was achieved by locating an individual electrospun fiber by AFM imaging and indenting with the AFM tip. A contact mode force-distance plot was achieved by pushing the AFM tip into the top of a PEO fiber and applying a force of around 50 nN. A cantilever spring constant K of 4.5 N m⁻¹ was used for imaging and nanomechanical testing, with the cantilever calibrated according to the method of Sader *et al.*¹⁰ Figure 2 shows a typical force-displacement curve produced when pushing the AFM tip into the PEO fiber and the subsequent removal of the tip at various temperatures. The loading curve shows how an increase in force is required to push the AFM tip into the fiber with the maximum indentation depth δ_m achieved at a maximum applied force F_m . The unloading curve differs from the loading curve due to the viscoelastic response of the fiber. The reduction of the applied force decreases the indentation depth until the applied force becomes negative, indicating (tensile) adhesion forces between the tip and the fiber during separation. Figure 2 (inset) indicates that the gradient of the unloading curve decreases as the heating temperature increases due to softening of the fiber sample. The elastic modulus of the fiber at the various temperatures studied can be calculated using analytical models of Sneddon¹¹ and Oliver and Pharr^{12,13} for indenting materials but modifying to account for the shape of the AFM tip as developed by Sirghi and Rossi.¹⁴ This modification shows that the AFM tip indentation depth δ is produced by a corresponding force $F(\delta)$ consisting of the externally applied force F_e and the adhesion force F_a , thus

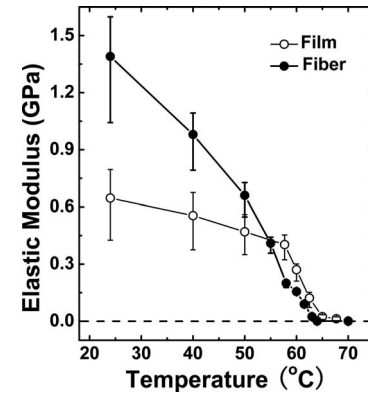


FIG. 3. Calculated elastic modulus of the PEO fiber and film from the experimental data fit of Eq. (1) as a function of temperature.

$$F(\delta) = F_e + F_a = \frac{2E_f \tan \alpha}{(1 - \nu_f^2)\pi} (\delta - \delta_r)^2 - \frac{\gamma_a \delta \tan \alpha}{\pi \cos \alpha} (\delta - \delta_r), \quad (1)$$

where E_f is the elastic modulus of the fiber, α is the half tip cone angle (taken as 11° from manufacturer's data), ν_f is the Poisson's ratio of the fiber [taken as 0.3 (Ref. 6)], γ_a is the thermodynamic work of adhesion, and δ_r is the AFM tip depth at $F=0$ on the unloading curve. An excellent fit of the recorded $F(\delta)$ with δ using Eq. (1) is shown in Fig. 2. The resultant calculated fiber elastic modulus E_f from Eq. (1) can therefore be plotted as a function of temperature, as shown in Fig. 3. The indentation of a solution cast PEO film is also shown in the same figure as a comparison. Small indentation depths approaching the radius of curvature of the AFM tip are better described using Hertz theory for a hemisphere contacting a surface.¹⁵ In this case, the obtained force-indentation depth curves are approximately linear at the lowest temperature (23 °C), and the resultant indentation data was calculated according to our previous work.¹⁶

Figure 3 indicates that the rate of elastic modulus drop with temperature dE_f/dT for the PEO film shows two regions. Initially dE_f/dT is small at less than 0.2 GPa from 20 °C to just before 60 °C, but then decreases rapidly at around 60 °C. This small elastic modulus decrease with temperature shows that the amorphous phase is continually softening with temperature, especially as the glass transition temperature of PEO is below room temperature. Melting of the crystal phase at T_m gives a more abrupt elastic modulus drop as seen in the second region. This therefore conforms to the behavior of a semicrystalline polymer. The thermomechanical response of the electrospun PEO fiber is somewhat different as the initial elastic modulus of the PEO fiber is much larger than that of the film. This is an important observation and highlights the increased molecular alignment from the electrospinning process. dE_f/dT for the electrospun fiber sample is almost constant from 20 °C to the T_m beyond 60 °C. As the magnitude of the drop in E_f with temperature is significant, the data presented here supports a mechanism where the electrospun fiber is anisotropic with a significant amorphous content but loses molecular alignment rapidly as the temperature is increased resulting in a corresponding decrease in E_f . The same mechanism has shown an abrupt decrease in the shear modulus of electrospun PS fibers at the glass transition in Ref. 17. This is unusual as polymer fibers

with significant structural anisotropy are generally highly crystalline.¹⁸ Therefore, the contribution of the amorphous phase to the elastic modulus of the fiber appears to dominate due to the almost constant loss of E_f with temperature. For the PEO film, loss in the elastic properties with temperature occurs at around 55 °C. This shows a direct correlation with the onset of the film melting peak in DSC (not shown), indicating that the mechanical properties of the film is dominated by crystal content in contrast to the electrospun fibers.

In conclusion, nMTA has been used to evaluate the thermomechanical properties of individual electrospun PEO fibers. Results show how the elastic modulus of PEO fibers is larger than corresponding films and indicates significant molecular orientation despite lower crystallinity. Thermomechanical response of individual electrospun fibers highlights a predominantly amorphous behavior with a gradual loss in mechanical properties with temperature.

This work was partially supported by the University of London Central Research Fund. Authors acknowledge NanoForce Ltd. and the NanoVision Centre at QMUL for using electrospinning and AFM facilities. Thanks are also give to Dr. M. Tian at NT-MDT, Europe BV for AFM measurement discussions.

- ¹J. Doshi and D. H. Reneker, *J. Electrostat.* **35**, 151 (1995).
- ²U. Singh, V. Prakash, A. R. Abramson, W. Chen, L. Qu, and L. Dai, *Appl. Phys. Lett.* **89**, 073103 (2006).
- ³Y. Dror, W. Salalha, R. L. Khalfin, Y. Cohen, A. L. Yarin, and E. Zussman, *Langmuir* **19**, 7012 (2003).
- ⁴E. P. S. Tan, C. N. Goh, C. H. Sow, and C. T. Lim, *Appl. Phys. Lett.* **86**, 073115 (2005).
- ⁵A. Arinstein, M. Burman, O. Gendelman, and E. Zussman, *Nat. Nanotechnol.* **2**, 59 (2007).
- ⁶M. Wang, H.-J. Jin, D. L. Kaplan, and G. C. Rutledge, *Macromolecules* **37**, 6856 (2004).
- ⁷J. M. Deitzel, J. D. Kleinmeyer, J. K. Hirvonen, and N. C. Beck Tan, *Polymer* **42**, 8163 (2001).
- ⁸S.-H. Ahn, J. H. An, D. S. Lee, and S. C. Kim, *J. Polym. Sci., Part B: Polym. Phys.* **31**, 1627 (1993).
- ⁹D. H. Reneker, A. L. Yarin, H. Fong, and S. J. Koombhongse, *J. Appl. Phys.* **87**, 4531 (2000).
- ¹⁰J. E. Sader, J. W. Chon, and P. Mulvaney, *Rev. Sci. Instrum.* **70**, 3967 (1999).
- ¹¹I. N. Sneddon, *Int. J. Eng. Sci.* **3**, 47 (1965).
- ¹²W. C. Oliver and G. M. Pharr, *J. Mater. Res.* **7**, 1564 (1992).
- ¹³G. M. Pharr, W. C. Oliver, and F. R. Brotzen, *J. Mater. Res.* **7**, 613 (1992).
- ¹⁴L. Sirghi and F. Rossi, *Appl. Phys. Lett.* **89**, 243118 (2006).
- ¹⁵K. L. Johnson, *Contact Mechanics* (Cambridge University Press, Cambridge, 1992), pp. 84–106.
- ¹⁶W. Wang, S. Li, and A. H. Barber, MRS Symposia Proceedings No. 1025, (Materials Research Society, Pittsburgh, 2007), p. B10–02.
- ¹⁷Y. Ji, B. Li, S. Ge, J. C. Sokolov, and M. H. Rafailovich, *Langmuir* **22**, 1321 (2006).
- ¹⁸A. P. Smith and H. Ade, *Appl. Phys. Lett.* **69**, 1833 (1996).